Critical components for diamond-based quantum coherent devices

Andrew D Greentree[1]**, Paolo Olivero**[2]**, Martin Draganski**[3]**,**
Elizabeth Trajkov[4]**, James R Rabeau**[2,4]**, Patrick Reichart**[2]**,**
Brant C Gibson[4]**, Sergey Rubanov**[2]**, Shane T Huntington**[4]**,**
David N Jamieson[1,2] **and Steven Prawer**[1,2,4]

[1] Centre for Quantum Computer Technology, School of Physics, The University of Melbourne,
Melbourne, Victoria 3010, Australia
[2] School of Physics, The University of Melbourne, Melbourne, Victoria 3010, Australia
[3] Applied Physics, RMIT University, GPO Box 2476V, Melbourne, Victoria 3001, Australia
[4] Quantum Communications Victoria, School of Physics, The University of Melbourne,
Melbourne, Victoria 3010, Australia

E-mail: andrew.greentree@ph.unimelb.edu.au

Abstract
The necessary elements for practical devices exploiting quantum coherence
in diamond materials are summarized, and progress towards their realization
documented. A brief review of future prospects for diamond-based devices is
also provided.

(Some figures in this article are in colour only in the electronic version)

1. Introduction

The quest to build a quantum computer is one of the most difficult and ambitious technological
challenges of the 21st century. It is difficult not just for technical reasons, but for fundamental
scientific reasons as well. These include the fact that quantum entanglement between large
numbers of particles, required for quantum computing [1], is still not fully understood.
But as we begin to understand entanglement and to engineer devices that exploit quantum
technology we will increase our knowledge of what it means along with our control of
entanglement. Even if some new no-go theorem is shown to preclude a scalable quantum
computer, quantum communication [2], quantum control [3–5], quantum key distribution [6, 7],
teleportation [8], entanglement-based frequency standards [9], quantum lithography [10], and
similar technologies are destined for central roles in science and technology. The purpose
of this review is to examine potential robust systems based on diamond, where the quantum
coherence can be interacted upon, stored, and then extracted into the outside world.

Diamond is an exceptional material. It is the hardest material; possesses the largest Young's modulus, the widest optical transparency window; is chemically inert; and can accommodate a wide variety of optically active colour centres (see for example Zaitsev [11]). Of these colour centres, one in particular, the nitrogen–vacancy (NV) centre, has attracted significant interest. Here we concentrate on the negatively charged version, the NV^- centre, and drop the negative sign except where there is potential ambiguity with the neutral NV^0 centre. Following the first detection of single NV centres using confocal microscopy [12], diamonds containing the NV colour centre have shown a number of useful properties: demonstration of a photo-stable single photon source at room temperature [13], demonstration of quantum key distribution (QKD) with pulsed true single photon pulses [14], observation of single spin measurement and coherent oscillations in a solid at room temperature [15], and demonstration of tomography of a solid-state (non-superconducting) qubit [16]. Furthermore, such features as multiply dressed states [17–19], electromagnetically induced transparency [20–22], and demonstration of two-qubit coupling [23] have also been reported. There are now many studies dealing with the structure of NV diamond, although a consensus of the exact mechanisms to describe the experimental phenomenology is still lacking (see [24, 25] and references therein). With the many promising attributes of NV diamond to date, it is likely that diamond will soon find applications in the exploitation of both quantum computing and quantum key distribution [26]. It is a further purpose of this review to examine the potential of diamond for such future applications.

The ability to synthesize high-quality diamond for optical applications has emerged in recent years. Combined with the ability to alter the physico-chemical properties of diamond by techniques such as irradiation and annealing, this has allowed engineered materials to be produced for specific applications. In particular, bulk single crystal samples containing controlled colour centres, especially the NV centre, are now available.

This opens the possibility of exploring the dynamics of single centres in diamond for their optical properties. An important recent development is demonstration of the growth of chemical vapour deposition (CVD) diamond films on pre-existing optical structures (e.g. optical fibres [27]); however, these devices are still inadequate for quantum computing applications, or for applications requiring more than one identical atom/photon. Issues of reproducibility, scalability, and optical transparency all need to be overcome before practical applications can be fully realized. These await the ability to engineer optically active centres at defined locations within photonic structures including waveguides and photonic bandgap cavities. Fabrication of these devices in diamond requires special techniques because of the extreme properties of diamond. As an example, the recently developed lift-off technique [28, 29], combined with single ion implantation [30, 31], has potential uses in the fabrication of diamond devices. Also required is the development of technology to selectively address individual centres, to controllably mediate interactions between individual centres, and to read out the quantum states of single centres. This review covers the challenge of bringing these devices to reality.

The solution to the placement problem is associated with another problem, ubiquitous to quantum systems of all types, but especially those in the solid state, namely particle distinguishability. Scalability of a quantum computer requires that the qubits (quantum bits, the equivalent of bits in classical computers) be distinguishable in some degree of freedom that is, in some sense, unbounded. The obvious degree of freedom is space, i.e. qubits are distinguished by their *position* within a quantum device. Concomitant with this is the need for their other parameters (e.g. transition energy, nearest neighbour coupling, and interactions with local control gates) to be as similar as possible. Such competing requirements immediately rule out many proposed implementations (e.g. homogeneous atomic groupings with inhomogeneously broadened spectral lines) as being ultimately unscalable, although they

may be useful in short-term applications. Liquid state NMR [33] is a prime example of an unscalable architecture which has nonetheless proved exceedingly useful in advancing the field (see for example [34]).

The spatial problem of creating atoms at well defined positions has been addressed in NV diamond [31], although there are outstanding issues regarding yield and placement accuracy. Associated with this is the technology to connect the different centres, which will be discussed below. However, the spectral inhomogeneity of NV centres would give rise to intolerable limitations on scalability without a reliable mechanism to tune the atoms to the same resonance. A method based on Stark shifting has long been proposed for this, and we will discuss this with regards to single centre work.

The quality of chemical vapour deposited diamond has been steadily improving over time due to the continuous efforts of many research groups, including Element 6, the worlds largest diamond manufacturer. One stringent measure of sample purity and perfection is the collection distance of electrical carriers in diamond which effectively measures the distance carriers can diffuse under the action of an electric field before recombination or scattering. The collection distance has increased from a few tens of microns for materials produced in the mid-1990s to nearly 1 mm today for the best materials. Extremely high carrier mobilities have been reported [32]. In addition, single crystal CVD diamond can now be grown with N concentrations from tens of ppm down to ppb levels.

This review is divided into three main sections. The first is a brief summary of some of the proposed implementations for diamond based quantum computing to highlight commonalities. The second section presents a method for fabricating microstructures within single crystal diamond with applications to the fabrication of practical diamond devices. The third section addresses the issue of creating individual NV centres in spatially defined locations.

2. Quantum computing architectures

There are at least five alternative proposals for entanglement generation, and quantum computing in NV diamond systems, of which three specifically use some properties of NV diamond, and two where NV diamond is merely a convenient system for their realization. Although it is not the purpose of this article to provide a comprehensive review of diamond-based quantum computing schemes, we will outline some of the proposals, so as to highlight some of the components necessary for each. Note that there are also many other schemes (e.g. cavity QED [35, 36], optically coupled quantum dot [37] and linear optical [38] schemes) that could be easily converted to NV diamond implementations. As will be seen, although many of the details are quite different, the actual structures required are very similar. Because of the central role played by Stark shifting in most NV based quantum computing schemes as a means for tuning centres into and out of resonance with each other and external optical fields, we will briefly discuss this issue separately. In addition to quantum computing, NV has been specifically suggested for other quantum device applications, including quantum repeaters [39] and as a quantum Q-switch [40]. Applications to QKD have been noted above.

Despite the continual improvements in diamond materials properties, it is highly unlikely that an entirely defect-free (ignoring the necessary defects that are used for qubits) material will ever be achievable. The issue for building large-scale quantum computers then becomes one of embracing the philosophy of *defect tolerance*. Rather than attempting to build a circuit in which every component works, a design is used where functioning elements (or equivalently non-functioning elements) are identified and connected to form an operating device. The problem of failure due to imperfections is then converted to the easier problem of routing.

The philosophy of defect tolerance is now beginning to be incorporated into proposed solid-state quantum computer architectures as a solution to the extreme demands imposed on qubits. The requirement for routing is in some sense addressed by flying qubits, identified by DiVincenzo's sixth and seventh criteria [41]. In many solid-state architectures, the identification of suitable flying qubits is problematic, but the 'optical handle' of the NV diamond system makes the use of photons as flying qubits very attractive. The defect-tolerant approach to quantum computing in NV diamond would then make use of controlled single centre, single photon interactions, and high fidelity transport of the flying qubits to mediate interactions between otherwise isolated NV centres. Given that there have already been demonstrations of single qubit [15] and two qubit [42] interactions that can satisfy the requirements for fault tolerance (ratio of gate time to coherence time of 10^{-4}) at room temperature despite the materials limitations, suggests that a defect tolerant approach should allow scalable qubit realizations in the near future. The repeat until success and weak nonlinearity-based schemes discussed below seem most suited to the defect tolerant approach, other schemes which need to be investigated in the NV paradigm include cavity-QED approaches [35, 36], the bus architecture of Spiller *et al* [43], and the operator-measurement-based scheme of Devitt *et al* [44].

2.1. Stark tuning of NV centres

The linear Stark shift is the change in the transition frequency of an electric dipole, when placed in an external electric field. It is written as

$$E_s = \vec{p} \cdot \vec{\mathcal{E}} \tag{1}$$

where $\vec{p}$ is the transition electric dipole moment, i.e. the difference in the dipole moments of the ground and excited states, and $\vec{\mathcal{E}}$ is the external applied electric field. The idea of using the Stark effect to shift transitions into resonance was introduced by Brewer and Shoemaker [45] as a new spectroscopic technique in their studies of molecules. Apart from finding application in a wide range of fields, it has also become a nearly ubiquitous part of NV based quantum computing, as it represents one mechanism for overcoming the inhomogeneous linewidth of NV diamond.

To recap the problem: the lifetime of the ^3E state (the first optically excited manifold) of NV diamond is around $T_1 = 12$ ns, depending on the exact sample and conditions [46], implying a linewidth of $\nu_h = 1/T_1 = 83$ MHz. However, in ensembles, the inhomogeneous linewidth (i.e. the linewidth arising from local perturbations to the optical transition frequency) is typically 750 GHz when measured below 100 K. Assuming that a randomly chosen centre will have a frequency somewhere within this distribution implies that all schemes based on optical coupling require some degree of tuning of the transitions so as to be either mutually resonant or significantly off-resonant with neighbouring centres, or some external control field. The Stark shift offers a potential solution.

To calculate the expected Stark shift in NV diamond, we note that an upper limit to the transition dipole moment of the NV centre is simply given by the charge (one electronic charge, q_e) separated by the atomic spacing of diamond $a = 0.15$ nm, and so the frequency shift per unit electric field felt by a centre aligned parallel to a uniform electric field can be easily determined by rearranging (1), i.e.

$$\frac{\nu_S}{\mathcal{E}} = \frac{q_e a}{h} = 3.6 \times 10^4 \text{ Hz (V m}^{-1})^{-1}, \tag{2}$$

where h is Planck's constant. This figure is, of course, an upper bound on the actual Stark shift, as it does not take into account effects such as screening of the electric field, and assumes
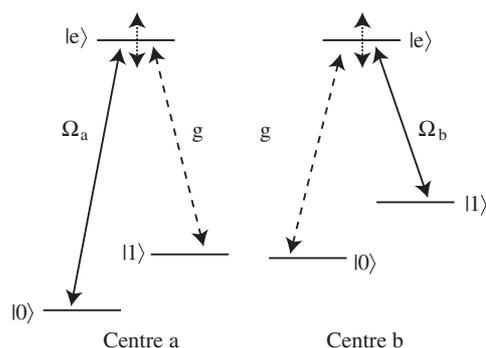
Figure 1. Scheme for resonant dipole–dipole interactions between two three level atoms. In each atom, the two photon transition can be mediated conditionally on the state of the other atom. The atom–atom coupling strength is either determined by the proximity of the atoms to each other, or can be long range if mediated by a cavity photon.

the largest possible charge separation. The Stark effect has been observed qualitatively in NV diamond several times previously [47, 48], although the canonical quantitative reference is from Redman *et al* [49]. In [49] a homogeneous sample of NV centres was prepared via persistent hole-burning, then a uniform electric field was applied, and its effect on the hole monitored. Although the centres in the spectral hole were homogeneous with respect to the transition frequency, they were not homogeneous with respect to the applied field, and so although one would expect the homogeneous line to split into eight different lines, in fact only a broadening of the line was observed. From this broadening it is possible to estimate the largest shift (corresponding to centres aligned parallel or anti-parallel with the field) as being

$$\frac{\nu_s}{\mathcal{E}} \sim 1 \times 10^4 \text{ Hz } (\text{V m}^{-1})^{-1}, \tag{3}$$

which is in passable agreement with the simple prediction above, at least until more precise single centre data is available.

Alternatively, we may calculate the electric field required to shift a centre by one inhomogeneous linewidth (∼750 GHz), which is of order 10^7 V m^{-1}, or 0.1 MV cm^{-1}. This field is significantly less than the field required to cause breakdown in single crystal diamond of 10 MV cm^{-1}, which is, incidentally, the largest of any known material [50].

2.2. Resonant dipole–dipole coupling

Two-qubit interactions have been proposed by using resonant dipole–dipole coupling to controllably entangle NV centres [51, 52]. The coupling exploits the Stark shift and the three-level nature of the NV centres to achieve Raman transitions that are conditional on the state of nearby centres. The idea can be understood with respect to figure 1.

Consider two atoms, *a* and *b*, in the Λ configuration, where the qubit states are the ground states, $|0\rangle$ and $|1\rangle$, and these are two photon coupled via the excited state $|e\rangle$. Two lasers are applied, one resonant (or quasi-resonant) with the $|0\rangle_a$–$|e\rangle_a$ transition with Rabi frequency Ω_a, and the $|1\rangle$–$|e\rangle$ transition coupled by a field with Rabi frequency Ω_b. In this arrangement, note that the frequencies of the $|e\rangle_a$–$|1\rangle_a$ and $|e\rangle_b$–$|0\rangle_b$ transitions are equal, so there will be an effective coupling between these transitions via virtual photon exchange if the atoms are in close proximity, or alternatively if the atoms communicate via a shared cavity mode that is initially unoccupied. This extra coupling, g, is state dependent and allows non-trivial phase shifts, and hence conditional quantum logic, to be performed, for example via conditional
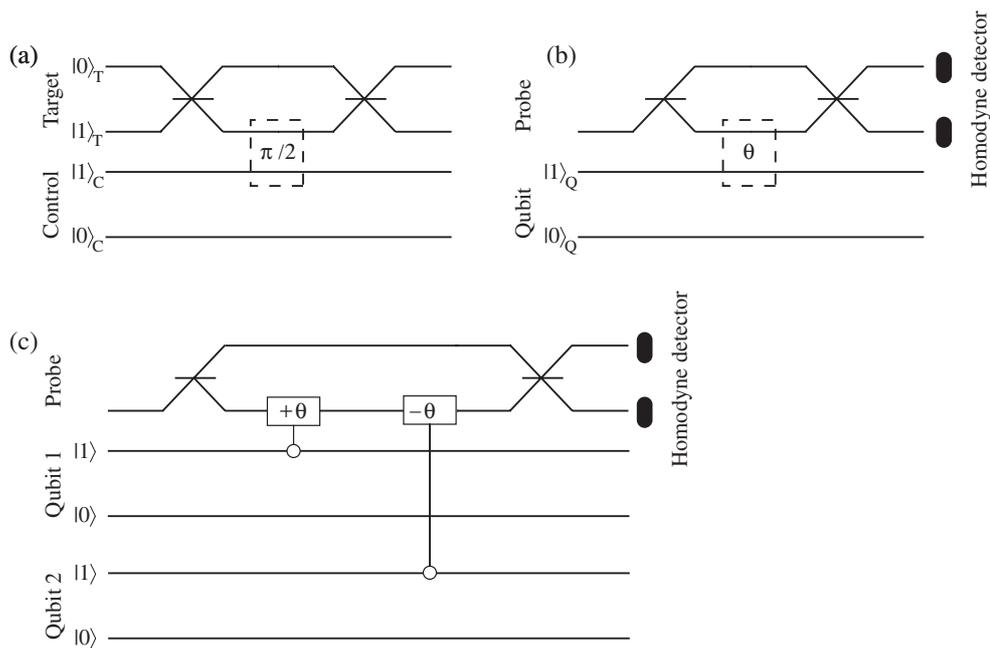
Figure 2. (a) Canonical scheme for CNOT operation with an ideal, lossless nonlinear medium (dotted box marked $\pi/2$) capable of providing a $\pi/2$ phase shift to the target, if the control photon is in the $|1\rangle$ state. (b) QND detector based on the weak nonlinearity scheme. A phase shift of $\theta \ll \pi/2$ is induced in the probe field by the presence or absence of a photon in the state $|1\rangle$, and this phase shift is detected by performing homodyne detection on the probe. (c) Parity gate exploiting the QND detector as a primitive. In this case the first interaction is a conditional phase shift of θ on the first qubit, and $-\theta$ from the second qubit. More complex schemes are possible, including CNOT gates, and hence universal quantum computation.

Raman adiabatic passage [51] or state information transfer between qubits via the shared channel [52]. Qubit selectivity is achieved by Stark tuning two atoms so that the required coupling schemes and resonances are achieved.

Ultimately, scalability in this scheme will be limited by issues such as the drop-off of the dipole–dipole coupling with distance, and ratio of homogeneous to inhomogeneous linewidth, or in the case of cavity-mediated interactions by the limited number of parallel operations that can be carried out (multiple occupation of the cavity will be problematic). Nevertheless, both schemes appear possible for of order 100 qubits, enough for convincing demonstrations, although we note that more than 100 qubits will be required for non-trivial quantum computing when error correction is required.

2.3. Weak nonlinearities

Historically, one of the earliest suggested implementations of a quantum gate was to use a material exhibiting a large, lossless Kerr-type nonlinearity in the path of an interferometer. Such an approach was outlined by Milburn [53], and has been expanded upon many times (see e.g. [54, 55]).

Conceptually, the approach to quantum computing via nonlinear optics is very simple. An interferometer is set up as shown in figure 2(a), where pairs of rails describe a qubit defined by a single photon in some superposition of each interferometer arm: dual rail notation. Essentially

the top pair of arms is a Mach–Zehnder interferometer with a Kerr-type nonlinear medium in one arm. It is balanced so that if zero or one photons pass through the nonlinear medium, the target photon leaves in the same state as it enters the interferometer. However, if the control photon in the state $|1\rangle_C$, then there is a phase shift such that the state of the target is reversed, realizing a controlled-NOT, CNOT, gate.

The essential problem with all such schemes, however, has been the lack of a suitable medium that can generate the required phase shift $(\pi/2)$ at the single photon level, without absorbing either control or target photon. Although there have been many suggestions for electromagnetically induced transparency (EIT) [56] and cavity-QED processes to generate the required nonlinearity [35], a somewhat surprising alternative has recently been proposed.

It was recently realized [57] that efficient photon counting quantum non-demolition (QND) detectors could be realized in a material exhibiting a weak, lossless nonlinearity, precisely the nonlinearity observed in EIT systems, without the requirement for a $\pi/2$ conditional phase shift. The device functions similarly to a high precision dark fringe interferometer. An interferometer is set up for a strong coupling field, aligned so that one output port sees a dark fringe; see figure 2(b). One arm of the interferometer has a cross-Kerr nonlinear medium, and the probe (to be detected) and one of the states of the qubit field pass through this medium. The weak nonlinearity induces a slight phase shift, θ, on the probe field, dependent on the presence or absence of photons in the qubit arm. This phase shift is detected by performing a homodyne measurement of the output light. Of course this phase shift will be extremely small; however, the signal will be proportional to both the phase shift and coupling intensity, effectively enhancing the weak nonlinearity.

The QND detector can be used as a primitive for more complex detectors, e.g. a parity detector for a two-qubit system (figure 2(c)). Here, the probe field acts as a bus, and with appropriate choice of applied nonlinear phases, effects coupling between different probe fields [58], and classical feedforward can be used to be project the qubits into the required states. Suitable choices of coupling and geometry permit a full Bell state analyser and near deterministic CNOT gate [59].

Although this approach can be applied to a large number of different implementations [43], NV diamond has a privileged place amongst optical/solid state implementations. The reason is that in order to amplify the (admittedly very small) lossless nonlinearities, very intense probe fields will need to be applied, which may tax materials properties such as melting point (for example in silica fibres). The fact that diamond has both the highest thermal conductivity and heat resistance therefore makes it the ideal choice for such implementations [60].

2.4. Repeat-until-success quantum computing

In principle, single qubit operations in NV diamond are relatively easy in either ensemble [61–63] or single centre [15] implementations. Despite measurements of NV-^{13}C [23] and NV–N coupling [64], as of writing, we are unaware of any unambiguous demonstrations of NV–NV coupling. Although there is no reason to suggest that this will not be possible, there are interesting alternative schemes, where qubit–qubit coupling can be achieved *without* direct two qubit interactions, using instead measurement-induced interactions.

The idea behind measurement-induced schemes is that individual qubits can be housed in separate cavities, and emitted photons from the cavities can be mixed on beam-splitters in a fashion so as to erase which-path information. In this way, conditional detection at beam-splitters projects the qubits onto entangled subspaces, with the exact entanglement generated being conditional on the measurement outcome. Two such schemes were introduced almost simultaneously, namely the 'repeat-until-success' scheme of Lim *et al* [65] and the 'double-

heralded' scheme of Barrett and Kok [66]. One of the very attractive features of both schemes is that if the protocol fails, then it can be repeated without any additional error to the overall quantum operation. The schemes are therefore highly suitable for the non-deterministic generation of entangled states, and indeed graph-state schemes along these lines have been proposed [67, 68].

Related to these non-deterministic, but heralded, schemes is a deterministic protocol that exploits the very powerful technique of operator measurements [69]. In these schemes a joint measurement of some two qubit operator is performed which is chosen to project the isolated matter qubits into an eigenstate which corresponds to an entangled subspace. Because the matter qubits are projected into an eigenstate, additional applications of the operator measurement simply project the qubits into the same eigenstate, hence the scheme is highly robust to loss of the detected photon. A scheme to realize such operator measurements in a highly general fashion (using the stabilizer formalism) has been presented [44], although that work was highly general and not specifically NV based.

2.5. Brokered graph state

Cluster states were originally proposed as an alternative paradigm for quantum computing in two-dimensional Ising lattices [70]; however, it is arguably true that it is in the field of linear optics quantum computing that their true utility has been identified [71–73]. The approach in [72] is especially interesting. In this scheme a mechanism for fusing cluster states is introduced that succeeds with 50% fidelity (shrinking the clusters with failure), so that appropriate choice of starting states is necessary for scalability (i.e. so that there is a net probability of increasing the size of the cluster state). This elegant proposal has been shown to dramatically decrease the overheads in terms of single photons to realize non-trivial quantum logic, over both the original KLM [38] and Nielsen [71] schemes.

Although it is obvious and natural to suggest that one-way quantum computing might be performed in NV diamond, it is far less easy to find a non-trivial implementation. A rather striking scheme has recently been proposed which is far from trivial, and uses NV centres (or systems with similar energy level schemes) in an essential fashion: brokered graph state quantum computing [74]. In this scheme entanglement between the 'brokers' is attempted (using, for example, the schemes described in section 2.4) and when successful (indicated by appropriate heralding) the entanglement is transferred to the clients. In the NV scheme, it is envisaged that the relatively easy to control electronic spins would be the brokers, and the well isolated nuclear spins would be the clients. Because the electron and nuclear spins can be effectively isolated unless interactions are desired, failure of the brokering does nothing to damage the existing client state entanglement.

3. Fabricating micro-structures in single crystal diamond

The very properties that make diamond so attractive as a material (especially hardness, and chemical inertness) make the micromachining of diamond extremely challenging [75–77]. Most existing techniques are based on the use of chemical vapour deposition (CVD) of polycrystalline films combined with selective ablation or replication processes that employ masking and moulding. Recently, sophisticated three-dimensional nano-structures were fabricated in nanocrystalline diamond [79, 80]. Although such structures have promising applications in micro-electromechanical system (MEMS) technology, single crystal diamond of sufficient levels of perfection to allow long decoherence times is required as the substrate for integrated quantum optics devices. This requirement arises from the necessity for identical
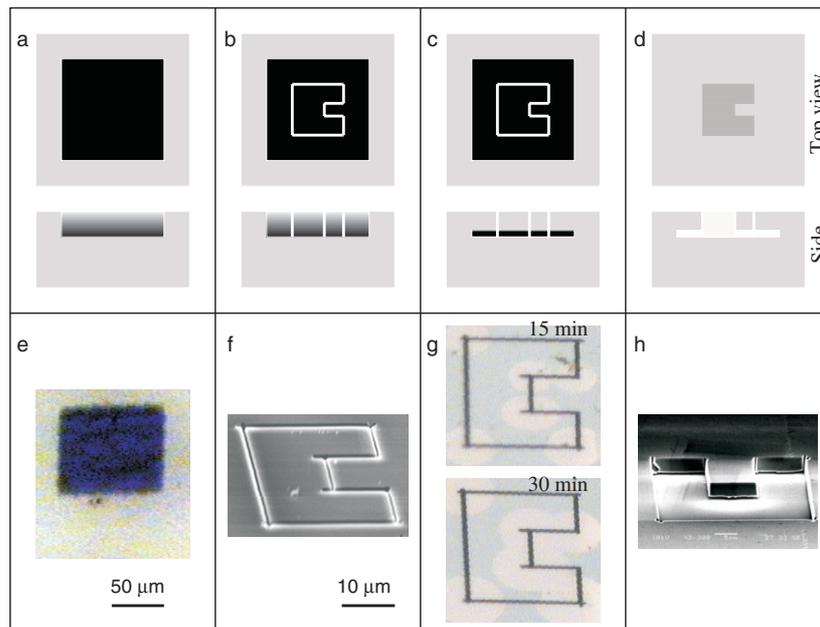
Figure 3. Schematic diagrams illustrating the FIB-assisted lift-off process ((a)–(d)). Single crystal diamonds are implanted with a 2 MeV He ion micro-beam in 100×100 μm^2 squares (a); then patterned with a FIB to expose in defined regions the buried sacrificial layer (b); thermal annealing turns the highly damaged regions into a selectively etchable material (c); upon etching, regions unconnected to the undamaged diamond lift off, leaving undercut microstructures in the diamond crystal (d). Images showing progress through the procedure ((e)–(g)). (e) Optical image of the MeV ion implanted region in diamond crystal, which is rendered opaque by the implantation. (f) SEM image of the FIB patterned area. (g) Optical images of the patterned region during progressive etching steps (after 15 and 30 min, respectively). (g) SEM image of the final (free-standing) structure after lift-off of the unconnected regions.

environments for each qubit. Combined with this is the fact that the optical quality of most CVD films is poor compared to that of silica or silicon.

A new method for the fabrication of free standing micro-structures in bulk single crystal diamond was recently demonstrated [29]. The method is inspired by the 'diamond lift-off' technique [28, 81], and takes advantage of the fact that, by means of ion implantation, it is possible to induce a phase transformation from diamond to a selectively etchable phase (the sacrificial layer). Here we briefly summarize the micro-fabrication process and report on the creation of a waveguide microstructure.

The sacrificial layer is created by the transformation induced by MeV ions which deposit most of their energy at the end of range, creating a spatially well defined disordered region (see schematic diagrams in figure 3(a) and optical microscopy image in figure 3(e)). The results demonstrated [29] employed 2 MeV He ions in synthetic high pressure high temperature (HPHT) diamond crystals, which created a 500 nm thick buried sacrificial layer located 3.5 μm below the surface. These conditions are by no means restrictive, and control of the energy, fluence, and implant species will all determine where most of the lattice transformation occurs; this has been studied in more depth previously [82–84]. Hence it is possible to control the vertical location of the sacrificial layer to sub-micron resolution [85].

To facilitate etching, the buried sacrificial layer must be exposed to the etchants, and hence some kind of milling must be employed. Laser ablation is one method [77, 78], but patterned
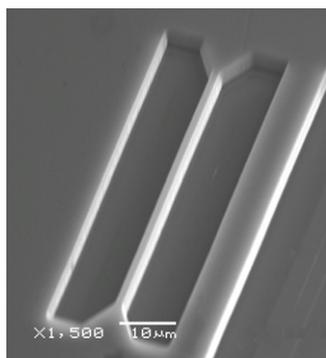
Figure 4. SEM image of a waveguide structure created in single crystal diamond with the FIB-assisted lift-off technique; the structure has a cross section of 3.5×2 μm^2, while the 500 nm undercut is visible.

milling with a focused ion beam (FIB) is our preferred method as the spatial resolution of the FIB is in principle much finer, allowing nanometre scale features to be drawn [86, 87] as shown schematically in figure 3(b) with the relevant SEM image in figure 3(f).

Thermal annealing is employed to convert the sacrificial layer to an etchable material with respect to the chemically inert diamond phase, while partially recovering the pristine diamond structure in volumes exposed to lower energy deposition. Wet chemical etching in boiling acid solution removes the exposed sacrificial layer, while leaving the diamond structure intact. This process is depicted schematically in figure 3(c), while figure 3(g) shows optical microscopy images of the sample at different stages of the etching process. Other efficient etching strategies, such as annealing in oxygen atmosphere [28, 81] or electrochemical etching [88], can also be employed. After selective etching, unconnected surface diamond layers lift off, leaving behind the desired patterned structure, which may include undercut regions, as shown in figure 3(d), together with the SEM image of the final structure in figure 3(h). A final thermal annealing step is also required to recover the pristine diamond structure from residual damage induced by both ion implantation and ion patterning.

A test structure comprising a free-standing bridge waveguide in single crystal diamond is shown in the SEM image in figure 4. With the same procedure, a range of three-dimensional structures (cantilevers, cavities, beam-splitters, etc) can be created in bulk diamond with sub-micrometre spatial resolution, and these are currently being investigated. The remarkable smoothness of the bottom surfaces after lift-off is due to the abrupt damage threshold for phase transformation upon annealing that leads to a sharp interface between diamond and the sacrificial layer, while the roughness of the lateral surfaces is defined by the accuracy and conditions of the FIB milling process, which can be significantly improved with vapour-assisted methods [89]. A more detailed description of the micromachining technique, together with an extensive characterization of the material properties of the structures during the fabrication process, can be found elsewhere [90].

4. Methods of implanting optically active centres in diamond

Ion implantation offers the possibility for the direct placement of NV centres in diamond with nanometre scale precision using technologies developed for the placement of single P donors in silicon [30]. However, unlike the case of silicon, for diamond, two alternative routes are available for the creation of NV centres.
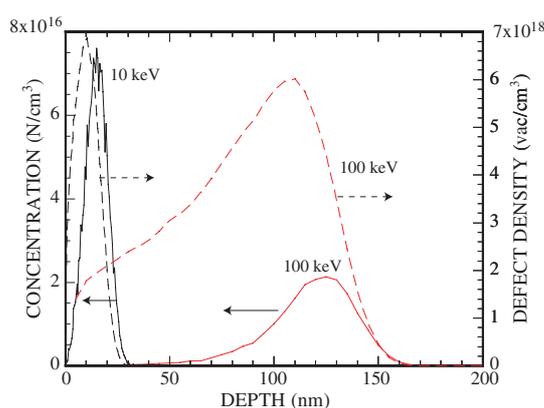
Figure 5. SRIM simulation of 10 and 100 keV N ions into diamond. A fluence of 1×10^{12} N cm^{-2} has been used in the simulations. The solid lines (scale on the left hand axis) is the N concentration due to the implanted ions. The dotted lines (scale on the right hand axis) show the corresponding vacancy concentration induced by the implanted N. Note that the vacancy concentration is about two orders of magnitude higher than the concentration of implanted N. Therefore unless ultrapure diamond is used, the probability that a native N will be converted to NV will exceed the probability that the implanted N will result in an NV centre.

The first method for NV creation involves implantation to create vacancies in nitrogen-rich type Ib diamond. Annealing above 600 °C causes the vacancies to migrate to the pre-existing substitutional nitrogen to form NV^0 and NV$^-$ centres. Exposure of diamond containing nitrogen to almost any kind of irradiation, followed by annealing above 550 °C, leads to formation of NV centres [91, 11], and specifically implantation of neutrons [92], protons, electrons, gallium [93], helium, carbon and other ions have all been employed for NV formation with this method. With this technique, NVs are formed from the nitrogen, so this method is best suited to creating ensembles or small ensembles of centres.

The second approach to NV formation involves the direct implantation of nitrogen ions into type IIa diamond containing low concentrations of nitrogen, followed by thermal annealing. This approach promises greater control of the absolute number of centres, down to the single centre level, which is necessary for the fabrication of arrays of single NV centres. Importantly, since one of the main causes of decoherence in NV centres is spin flips due to the presence of excess nitrogen spins (and to a lesser extent, background ^{13}C, and we note that pure ^{12}C is available for ultra-heat sinking applications) [62], the use of high purity crystals is essential to increase decoherence times.

An important parameter for the scalability of fabricating arrays of NV centres by ion implantation is the probability that a single implanted nitrogen will result in an observable and usable NV centre. Nitrogen has been implanted into diamond to create NV centres previously [94, 31]. Perhaps surprisingly, however, the measurement of the conversion efficiency of *implanted* nitrogen to NV is difficult and not resolved in the previous works. In order to understand the problem, we present in figure 5 the results of a SRIM [95] simulation of the implantation of 10 and 100 keV N atoms into diamond. Note that for each implanted N, more than 80 and 300 vacancies are produced for 10 and 100 keV implantations respectively. Consequently there is a high probability that any pre-existing nitrogen near or within the track of the implanted ion will be in close proximity to a vacancy, and hence be converted into an NV centre upon annealing. Therefore if the direct N implantation approach is adopted, a background nitrogen concentration of less than approximately 7 and 0.05 ppm for 10 and
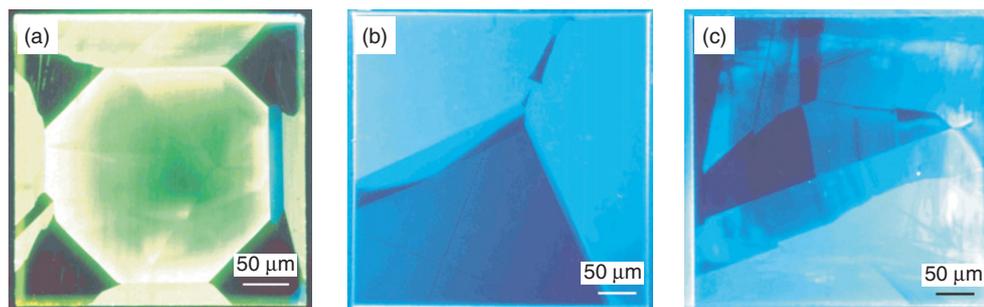
Figure 6. Cathodoluminescence maps of type Ib HPHT (100) crystal (a) and type IIA HPHT diamonds sourced from Sumitomo Diamond Corporation. (b) (100) and (c) (111) crystals; although all three samples are mono-crystalline, growth sectors are clearly visible in all crystals. The sectors exhibit different luminescence properties, reflecting their differing impurity and defect compositions. Each individual diamond displays a unique sector signature which must be taken into account when considering the effect of implantation.

100 keV implants respectively is required to avoid the native N swamping any implanted N. (The higher energy implants affect a much larger volume of material hence to ensure that on average there are very few native N in the affected volume a lower background N concentration is required.) Hence measuring the probability that an implanted N will result in a single NV being created is complicated. As explained below, this problem can be addressed by the implantation of ^{15}N and the detection of ^{15}NV, which, via the hyperfine splitting, can be distinguished from ^{14}NV centres [96]. We now discuss each method in turn.

4.1. Direct implantation of vacancies

As stated above, the implantation of even low fluences of inert ions can result in the formation of NV centres due to the 'activation' of nitrogen in the sample. In this case it is clear that the resultant NV concentration will depend primarily on the pre-existing N concentration within the track of the implanted ion. In this regard it is important to note that N is often not uniformly distributed throughout a sample. Figure 6(a) is a flood cathodoluminescence (CL) map of a high pressure high temperature Sumitomo type Ib diamond. Strong growth sectoring is clearly evident and is thought to arise from the fact that the diamond crystals grow out from a single seed. The growth sectors have been imaged in CVD single crystals by TEM [97]. Raman spectroscopy [98] has shown that the different growth sectors (mainly (100) and (111)) also contain different levels of defects. The probability of incorporation of impurities and defects is, in general, higher for the (111) than (100) growth sectors. The results of ion irradiation implantation will therefore depend on which sector is implanted. Because the sectoring is often not evident under an optical microscope, experimentalists are often unaware of the spatial inhomogeneity of the nitrogen concentration. Moreover, there is often inhomogeneity in the incorporation of other impurities (e.g. Ni or vacancies) as well as strain fields set up by the sector boundaries. This may result in lack of reproducibility between reported results, and needs to be taken into account in all measurements on such sectored samples. Strong sectoring is also apparent in Sumitomo diamonds which have a low native concentration of N (figures 6(b) and (c)).

To explore of the use of vacancy creation in type 1b samples, squares of area $50 \times 50 \ \mu\mathrm{m}^2$ were irradiated with 30 keV Ga ions ($R_\mathrm{p} \pm \Delta R_\mathrm{p} = 15 \pm 3$ nm, where R_p is the projected range) using a focused ion beam, over a wide range of fluences from 1×10^9 to 1×10^{18} ions cm^{-2}.
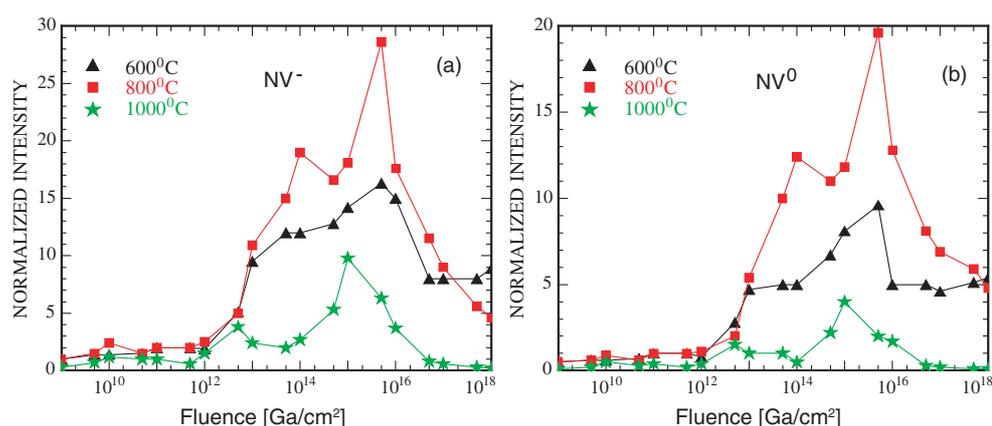
Figure 7. The intensity of (a) the NV^- (637 nm) and (b) the NV^0 (575 nm) ZPL normalized to the intensity of the first order Raman mode (at 1332 cm^{-1}) as a function of Ga ion fluence. The Ga ion energy was 30 keV. Data for post-implantation annealing at 600, 800, and 1000 °C are shown. The PL was excited by 514 nm excitation and the spectra collected at 77 K.
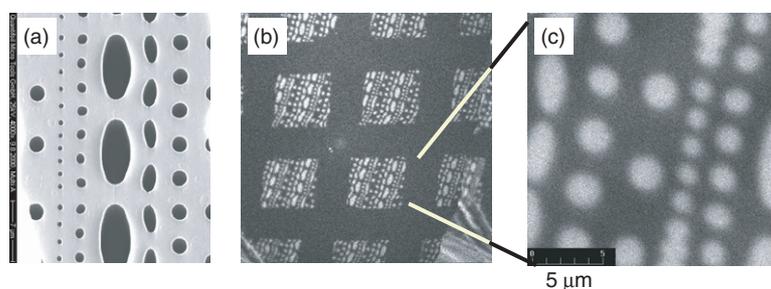

Figure 8. Patterning of NV centres in type Ib diamond via implantation through a mask. (a) The quantifoil carbon grid used to mask the sample during ion implantation. The grid was coated with Au to increase the stopping power. Confocal luminescence imaging ((b) and (c)) shows that the mask pattern is faithfully transferred to the sample.

The sample employed was a type Ib HPHT diamond and care was taken to perform all the irradiations within the same sector. The sample was isochronally annealed from 200 to 1000 °C for 1 h in an argon atmosphere.

Figure 7 shows the intensity of the NV^0 and NV^- zero phonon lines (ZPLs) normalized to the intensity of the first order bulk Raman line as a function of ion fluence for samples annealed at 600, 800, and 1000 °C (note that vacancies only become mobile above 550 °C [99]). From measurements of the normalized intensity versus ion fluence and annealing temperature, it may be inferred that for the most intense NV emission the optimal annealing temperature is about 800 °C and the optimal fluence about 5×10^{15} Ga cm^{-2}. This fluence corresponds to about one monolayer, i.e. to complete coverage by the Ga beam of the entire surface. Since each Ga impact creates more than 250 vacancies per incident ion, it is not surprising that the saturation of NV production occurs when, on average, the entire irradiated area has been impacted by at least one Ga ion. Note, however, that the optimal conditions for maximum intensity do not necessarily correspond to optimal quantum optical properties of the centres thus produced. For example, the ZPL FWHM of the centres at high Ga fluences is much larger than those formed at low fluences.
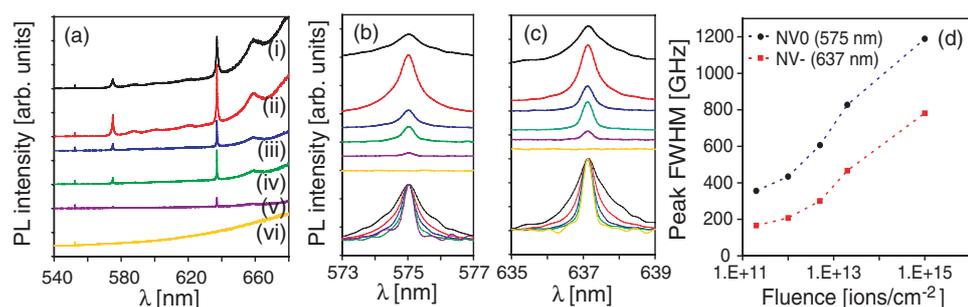
Figure 9. (a) Photoluminescence spectra from regions implanted at varying ion fluences into high quality type IIa diamond crystal. The fluences were (i) 1×10^{15} N cm^{-2}, (ii) 2×10^{13} N cm^{-2}, (iii) 5×10^{13} N cm^{-2}, (iv) 1×10^{12} N cm^{-2}, (v) 2×10^{11} N cm^{-2}, and (vi) 2×10^{10} N cm^{-2}. All spectra are normalized to the intensity of the first order diamond Raman line and displaced vertically for clarity. (b), (c) Zoom spectra of NV^0 and NV$^-$ zero phonon lines, respectively; in the bottom part of the graph, the spectra are overlaid to emphasize the monotonic sharpening of the peaks with decreasing ion fluences. (d) The width of the NV^0 and NV$^-$ zero phonon lines in frequency units, as a function of the ion fluences.

By performing ion implantation through a micron-scale mask, the damage will be localized to the regions exposed to the ion beam, and hence arrays of NV centres will be produced. A fluorescence image showing an NV array generated by this method is shown in figure 8. The fluorescence was imaged using a confocal microscope. Although the bright spots in figure 8 are clusters, rather than single NV centres, the result proves that such arrays can be created quickly and easily in diamond. Scaling this to single NV can be accomplished by irradiating through nano-scale, rather than micron-scale, masks. For example, if the irradiation is performed through a 20 nm aperture, and assuming a background N concentration of 1 part per million, on average about one NV centre will be created per aperture. Following the implantation, transparent conducting electrodes (e.g. ZnO, ITO) can be deposited through the masks to create electrical contacts registered to the single NV centres. Such registration is necessary for Stark shift tuning of individual NV centres (see section 2.1).

It should be recognized that this technique does not allow for precise control of the number of centres in a given spot, and will produce, at best, pseudo-ordered arrays in which locations on the array will have a (small) number of NV centres determined by Poissonian statistics. Nevertheless, it does allow rapid testing of many key parameters, such as, for example, the registering of transparent electrodes to small clusters, and the refinement of the optical detection techniques. Given the relative ease of identifying NV centres, post-selection on centres with the required characteristics may be a viable option for many applications.

4.2. Direct implantation of single nitrogen ions

In principle, deterministic control of the number of NV centres in a given region can be obtained by the implantation of single nitrogen atoms or molecular dimers directly into high quality diamond with little or no N background. As mentioned above, extremely high quality material with N concentrations of <10 ppb have been fabricated [32]. Basic concerns have been raised that this technique will result in too much residual damage to allow for the reliable fabrication of a single qubit. However, as a demonstration of the effectiveness of the scheme, N$_2$ has been implanted at extremely low fluences into very low nitrogen content diamond. Figure 9 shows a plot of the ZPL for various fluences of 14 keV N with the inset showing the

FWHM as a function of N concentration. In this case the maximum possible NV concentration corresponds to the implanted N concentration. For ensemble measurements it would appear that NV concentrations as low as 1×10^{18} NV cm^{-3} are quite easily resolved. As shown in figure 9(d), the width of the zero phonon line emission decreases monotonically with decreasing ion fluence, while an optimal ion fluence of 2×10^{13} ions cm^{-2} determines the maximum intensity of the peak.

For the fabrication of qubits via direct N implantation, it is desirable that each implanted N creates a single NV, and that there is no excess N. Hence the probability of forming an NV centre under these conditions must be known. This is difficult because it is not obvious how to distinguish between native and implanted NVs in photoluminescence. However, by implanting single ^{15}N ions instead of ^{14}N, a mechanism is available to measure the yield [96]. ^{15}N is a spin 1/2 nucleus and, therefore, ^{15}NV has a different hyperfine spectrum from ^{14}NV (which is a spin 1 nucleus). Because the natural abundance of ^{15}N is 0.37%, the observation of ^{15}NV at fractions greater than this provides a clear spectral signature of their origin. Initial measurements [96] in unoptimized conditions indicate that approximately 2.5% of implanted ions gave rise to optically observable NV centres, all of those measured being ^{15}NV. The experimental conditions for that work had not been optimized, and we expect further developments (e.g. cold implantation [99], or optimal implant energies [31]) to improve yields further.

5. Conclusions

The motivation for the use of diamond in quantum computing lies primarily in the availability of an 'optical handle', i.e. a reliable and robust optical method for single spin read-out and qubit control. The NV centre in diamond is a strong candidate for a solid-state qubit operating at room temperature. The optical handle gives other possibilities as well, however, as it allows for the generation of entangled photons, increasing the utility of 'stepping-stone' devices, *en route* to full blown quantum computing.

However, to translate this potential into usable devices requires the development of a nanofabrication toolkit for diamond. Specifically, the key elements needed to engineer qubits in diamond require (i) sourcing and characterizing materials of sufficient purity, (ii) the ability to pattern individual NV centres in diamond and register them to electrical gates, (iii) the ability to tune the optical output of a single NV using the Stark shift, (iv) the ability to fabricate waveguide input–output mirrors in single crystal diamond and (v) establishing the capability for coupling the NV centres to cavities/photonic bandgap structures. Excellent progress has been made on all fronts. Ion implantation techniques seem ideally suited to the controlled creation of NV centres in diamond. To combine these qubits into a full quantum architecture will require further development and application of the philosophy of defect tolerance in the architecture: an approach that NV diamond appears especially suited to. The lift-off technique has been shown to be capable of creating waveguides, mirrors and other optical structures. Preliminary data shows that it will be possible to Stark shift tune individual NV centres into resonance, and provided that the required surface roughness can be attained it should be possible to use a combination of lift-off and FIB techniques to create photonic bandgap cavities in diamond. Finally, sophisticated, but entirely realizable primitives and architectures have been theoretically modelled that provide guidance to the sort of interesting structures and devices which can be fabricated in the near future.

Acknowledgments

References

[1] Blume-Kohout R, Caves C M and Deutsch I H 2002 *Found. Phys.* **32** 1641
[2] Davies E B 1977 *IEEE Trans. Inform. Theory* **23** 530
[3] Belavkin V P 1983 *Autom. Remote Control* **44** 178 (Engl. Transl.)
[4] Wiseman H M and Milburn G J 1993 *Phys. Rev. Lett.* **70** 548
[5] Rabitz H, de Vivie-Riedle R, Motzkus M and Kompa K 2000 *Science* **288** 824
[6] Bennett C H and Brassard G 1984 *Proc. IEEE Int. Conf. Computers, Systems and Signal Processing* (Piscataway, NJ: IEEE) p 175
[7] Ekert A K 1991 *Phys. Rev. Lett.* **67** 661
[8] Bennett C H, Brassard G, Crpeau C, Jozsa R, Peres A and Wootters W K 1993 *Phys. Rev. Lett.* **70** 1895
[9] Huelga S F, Macchiavello C, Pellizzari T, Ekert A K, Plenio M B and Cirac J I 1997 *Phys. Rev. Lett.* **79** 3865
[10] Boto A N, Kok P, Abrams D S, Braunstein S L, Williams C P and Dowling J P 2000 *Phys. Rev. Lett.* **85** 2733
[11] Zaitsev A M 2001 *Optical Properties of Diamond: A Data Handbook* (Berlin: Springer)
[12] Gruber A, Dräbenstedt A, Tietz C, Fleury L, Wrachtrup J and von Borczyskowski C 1997 *Science* **276** 2012
[13] Beveratos A, Kühn S, Brouri R, Gacoin T, Poizat J-P and Grangier P 2002 *Eur. Phys. J.* D **18** 191
[14] Beveratos A, Brouri R, Gacoin T, Villing A, Poizat J-P and Grangier P 2002 *Phys. Rev. Lett.* **89** 187901
[15] Jelezko F, Gaebel T, Popa I, Gruber A and Wrachtrup J 2004 *Phys. Rev. Lett.* **92** 076401
[16] Howard M, Twamley J, Wittmann C, Gaebel T, Jelezko F and Wrachtrup J 2006 Quantum process tomography and Linblad estimation of a solid-state qubit *New J. Phys.* **8** 33
[17] Greentree A D, Wei C, Holmstrom S A, Martin J P D, Manson N B, Catchpole K R and Savage C 1999 *J. Opt. B: Quantum Semiclass. Opt.* **1** 240
[18] Wei C, Holmstrom S A, Greentree A D and Manson N B 1999 *J. Opt. B: Quantum Semiclass. Opt.* **1** 289
[19] Greentree A D, Wei C and Manson N B 1999 *Phys. Rev.* A **59** 4083
[20] Wei C and Manson N B 1999 *J. Opt. B: Quantum Semiclass. Opt.* **1** 464
[21] Wilson E A, Manson N B and Wei C 2003 *Phys. Rev.* A **67** 023812
[22] Santori C, Fattal D, Spillane S M, Fiorentino M, Beausoleil R G, Greentree A D, Olivero P, Draganski M, Rabeau J R, Reichart P, Gibson B C, Rubanov S, Huntington S T, Jamieson D N and Prawer S 2006 Coherent population trapping in diamond N–V centers at zero magnetic field *Preprint* cond-mat/0602573
[23] Jelezko F, Gaebel T, Popa I, Domhan M, Gruber A and Wrachtrup J 2004 *Phys. Rev. Lett.* **93** 130501
[24] Wrachtrup J and Jelezko F 2006 Quantum information processing in diamond *J. Phys.: Condens. Matter* **18** S807 (*Preprint* quant-ph/0510152)
[25] Manson N B, Harrison J P and Sellars M J 2006 The nitrogen–vacancy center in diamond re-visited *Preprint* quant-ph/0601360
[26] ARDA Roadmap 2004 http://qist.lanl.gov
[27] Rabeau J R, Huntington S T, Greentree A D and Prawer S 2005 *Appl. Phys. Lett.* **86** 134104
[28] Parikh N R, Hunn J D, McGucken E, Swanson M L, White C W, Rudder R A, Malta D P, Posthill J B and Markunas R 1992 *Appl. Phys. Lett.* **61** 3124
[29] Olivero P, Rubanov S, Reichart P, Gibson B C, Huntington S T, Rabeau J R, Greentree A D, Salzman J, Moore D, Jamieson D N and Prawer S 2005 *Adv. Mater.* **17** 2427
[30] Jamieson D N, Yang C, Hopf T, Hearne S M, Pakes C I, Prawer S, Mitic M, Gauja E, Andresen S E, Hudson F E, Dzurak A S and Clark R G 2005 *Appl. Phys. Lett.* **86** 202101
[31] Meijer J, Burchard B, Domhan M, Wittmann C, Gaebel T, Popa I, Jelezko F and Wrachtrup J 2005 *Appl. Phys. Lett.* **87** 261909
[32] Isberg J, Hammersberg J, Johansson E, Wikstrom T, Twichen D J, Whitehead A J, Coe S E and Scarsbrook G A 2002 *Science* **297** 1670
[33] DiVincenzo D P 1995 *Phys. Rev.* A **51** 1015

[34] Chuang I L, Vandersypen L M K, Zhou X, Lueng D W and Lloyd S 1998 *Nature* **393** 143
[35] Turchette Q A, Hood C J, Lange W, Mabuchi H and Kimble H J 1995 *Phys. Rev. Lett.* **75** 4710
[36] Cirac J I, Zoller P, Kimble H J and Mabuchi H 1997 *Phys. Rev. Lett.* **78** 3221
[37] Lovett B W, Reina J H, Nazir A and Briggs G A D 2003 *Phys. Rev.* B **68** 205319
[38] Knill E, Laflamme L and Milburn G J 2001 *Nature* **409** 46
[39] Childress L, Taylor J M, Sørensen A S and Lukin M D 2006 *Phys. Rev. Lett.* **96** 070504
[40] Greentree A D, Salzman J, Prawer S and Hollenberg L C L 2006 Quantum gate for Q switching in monolithic photonic-band-gap cavities containing two-level atoms *Phys. Rev.* A **73** 013818
[41] DiVincenzo D P 2000 *Fortschr. Phys.* **48** 771
[42] Gaebel T *et al* 2006 Room temperature coherent control of coupled single spins in a solid, submitted
[43] Spiller T P, Nemoto K, Braunstein S L, Munro W J, van Loock P and Milburn G J 2006 Quantum computation by communication *New J. Phys.* **8** 30
[44] Devitt S J, Greentree A D and Hollenberg L C L 2005 Information free quantum bus for universal quantum computation *Preprint* quant-ph/0511084
[45] Brewer R G and Shoemaker R L 1971 *Phys. Rev. Lett.* **27** 631
[46] Collins A T, Thomaz M F and Jorge M I B 1983 *J. Phys. C: Solid State Phys.* **16** 2177
[47] Kaplyans A A, Kolyshki V I and Medvedev V N 1970 *Sov. Phys.—Solid State* **12** 1193
[48] Davies G and Manson N B 1980 *Ind. Diamond Rev.* **50** 1980
[49] Redman D, Brown S and Rand S C 1992 *J. Opt. Soc. Am.* B **9** 768
[50] Geis M W, Efremow N N and Rathman D D 1988 *J. Vac. Sci. Technol.* A **6** 1953
[51] Lukin M D and Hemmer P R 2000 *Phys. Rev. Lett.* **84** 2818
[52] Shahriar M S, Hemmer P R, Lloyd S, Bhatia P S and Craig A E 2002 *Phys. Rev.* A **66** 032301
[53] Milburn G J 1989 *Phys. Rev. Lett.* **62** 2124
[54] Chuang I L and Yamamoto Y 1995 *Phys. Rev.* A **52** 3489
[55] Gerry C C 1999 *Phys. Rev.* A **59** 4095
[56] Harris S E, Field J E and Imamoğlu A 1990 *Phys. Rev. Lett.* **64** 1107
[57] Munro W J, Nemoto K, Beausoleil R G and Spiller T P 2005 *Phys. Rev.* A **71** 033819
[58] Munro W J, Nemoto K, Spiller T P, Barrett S D, Kok P and Beausoleil R G 2005 *J. Opt. B: Quantum Semiclass. Opt.* **7** S135
[59] Nemoto K and Munro W 2005 *Phys. Rev. Lett.* **93** 250502
[60] Munro W J 2005 private communications
[61] Charnock F T and Kennedy T A 2001 *Phys. Rev.* B **64** 041201(R)
[62] Kennedy T A, Charnock F T, Colton J S, Butler J E, Linares R C and Doering P J 2002 *Phys. Status Solidi* **233** 416
[63] Kennedy T A, Colton J S, Butler J E, Linares R C and Doering P L 2003 *Appl. Phys. Lett.* **83** 4190
[64] Gaebel T *et al* 2006 in preparation
[65] Lim Y L, Beige A and Kwek L C 2005 *Phys. Rev. Lett.* **95** 030505
[66] Barrett S D and Kok P 2005 *Phys. Rev.* A **71** 060310(R)
[67] Benjamin S C, Eisert J and Stace T M 2005 *New J. Phys.* **7** 194
[68] Lim Y L, Barrett S D, Beige A, Kok P and Kwek L C 2006 *Phys. Rev.* A **73** 012304
[69] Nielsen M A and Chuang I L 2000 *Quantum Computation and Quantum Information* (Cambridge: Cambridge University Press)
[70] Raussendorf R and Briegel H J 2001 *Phys. Rev. Lett.* **86** 5188
[71] Nielsen M A 2004 *Phys. Rev. Lett.* **93** 040503
[72] Browne D E and Rudolph T 2005 *Phys. Rev. Lett.* **95** 010501
[73] Walther P, Resch K J, Rudolph T, Schenck E, Weinfurter H, Vedral V, Aspelmeyer M and Zeilinger A 2005 *Nature* **434** 169
[74] Benjamin S C, Browne D E, Fitzsimons J and Morton J J L 2005 Brokered graph state quantum computing *Preprint* quant-ph/0509209
[75] Björman H, Rangsten P and Hjort K 1999 *Sensors Actuators* **78** 41
[76] Fu Y and Du H J 2001 *Proc. SPIE* **4557** 24
[77] Ramanathan D and Molian P A 2002 *J. Manuf. Sci. Eng.* **124** 389
[78] Hunn J D and Christensen C P 1994 *Solid State Technol.* **37** 57
[79] Sekaric L, Parpia J M, Craighead H G, Feygelson T, Houston B H and Butler J E 2002 *Appl. Phys. Lett.* **81** 4455
[80] Auciello O, Birrell J, Carlisle J A, Gerbi J E, Xiao X, Peng B and Espinosa H D 2004 *J. Phys.: Condens. Matter* **16** R539
[81] Hunn J D, Withrow S P, White C W, Clausing R E, Heatherly L, Christensen C P and Parikh N R 1995 *Nucl. Instrum. Methods Phys. Res.* B **99** 602

[82] Prawer S 1995 *Diamond Relat. Mater.* **4** 862
[83] Prawer S and Kalish R 1995 *Phys. Rev.* B **51** 15711
[84] Orwa J O, Nugent K W, Jamieson D N and Prawer S 2000 *Phys. Rev.* B **62** 5461
[85] Breese M B H, Jamieson D N and King P J C 1996 *Material Analysis Using a Nuclear Microprobe* (New York: Wiley)
[86] Karlsson M and Nikolajeff 2003 *Opt. Express* **11** 502
[87] Fu Y and Bryan N K A 2003 *Opt. Eng.* **42** 2214
[88] Marchywka M, Pehrsson P E, Binari S C and Moses D 1993 *J. Electrochem. Soc.* **140** L19
[89] Adams D P, Vasile M J, Mayer T M and Hodges V C 2003 *J. Vac. Sci. Technol.* B **21** 2334
[90] Olivero P, Rubanov S, Reichart P, Gibson B C, Huntington S T, Rabeau J R, Greentree A D, Salzman J, Moore D, Jamieson D N and Prawer S 2006 *Diamond Relat. Mater.* at press doi:10.1016/j.diamond.2006.01.018
[91] Nishida Y, Mita Y, Mori K, Okuda S, Sato S, Yazu S, Nakagawa M and Okada M 1989 *Mater. Sci. Forum* **38–41** 561
[92] Mita Y 1996 *Phys. Rev.* B **53** 11360
[93] Martin J, Wannemacher R, Teichert J, Bischoff L and Köhler B 1999 *Appl. Phys. Lett.* **75** 3096
[94] Kalish R, Uzan-Saguy C, Philosoph B, Richter V, Lagrange J P, Gheeraert E, Deneuville A and Collins A T 1997 *Diamond Relat. Mater.* **6** 516
[95] Ziegler J F, Biersack J P and Littmark U 1985 *The Stopping and Range of Ions in Solids* (New York: Pergamon)
[96] Rabeau J R, Reichart P, Tamanyan G, Jamieson D N, Prawer S, Jelezko F, Gaebel T, Popa I, Domhan M and Wrachtrup J 2006 *Appl. Phys. Lett.* **88** 023113
[97] Tarutani M, Shimato Y, Takai Y and Shimizu R 1995 *Appl. Phys. Lett.* **67** 632
[98] Nugent K W and Prawer S 1998 *Diamond Relat. Mater.* **7** 215
[99] Prins J F 1988 *Phys. Rev.* B **38** 5576